Transport in Porous Media **8**: 133–147, 1992.

Implication of Fractal Geometry for Fluid Flow Properties of Sedimentary Rocks

J. MULLER and J. L. McCAULEY
Institutt for energiteknikk, Box 40, 2007-Kjeller, Norway

(Received: 19 April 1990; in final form: 7 March 1991)

Abstract. It is demonstrated that a certain amount of order can be extracted from an apparently random distribution of pores in sedimentary rocks by exploiting the scaling characteristics of the geometry of the porespace with the help of fractal statistics. A simple fractal model of a sedimentary rock is built, and is tested against both the Archie law for conductivity and the Carman–Kozeny equation for permeability. We demonstrate how multifractal scaling of pore-volume can be used as a tool for rock characterization by computing its experimental $f(\alpha)$ spectrum, which can be modelled by a simple two-scale Cantor set.

Key words. Fractal, multifractal, sedimentary rocks, permeability.

1. Introduction

The description of the porespace of sedimentary rocks and their fluid flow properties is a complex problem which has been generally avoided by physicists and only empirically modelled by reservoir engineers. The recent advances in 'new-physics' have given us the possibilities to attack problems formulated as complicated differential equations (such as the Navier–Stokes) by new, nontraditional, methods that are based on solutions of iterative maps. These methods are applied to systems whose limiting solutions (of differential equations) are *not* smooth differentiable curves. Examples of such systems are, amongst others, fluid flow through a sedimentary rock, turbulence, and the growth of objects of irregular shape (such as snowflakes). The characteristics of these 'noisy' jagged curve is their fractal shape described by Mandelbrot in his *Fractal Geometry of Nature* [1].

In what follows, we shall not discuss derivations or solutions of iterative maps [2]. Instead, we demonstrate how a simple fractal model can give us an understanding of the fluid flow and the conductivity properties of a porous medium in terms of empirical relations such as the known Carman–Kozeny [3] and Archie laws [4].

The paper is organized as follows. In Section 2, we discuss some fundamental properties of fractal objects and explain how we measure those properties. Our fractal model is described in Section 3, where we show its strength and weakness by comparison with other existing models. The concept of multifractals, which plays a leading role in extracting order from apparent randomness in nature, is introduced in Section 4. We demonstrate how multifractals can be used as a tool for rock

characterization and point out their significance in making realistic models of porous media for predictions of fluid flow. Concluding remarks are the subject of Section 5.

2. Fractals – Major Characteristics and Their Measurements

Fractal geometry [1] is a tool for characterizing objects occuring in nature. It differs from the Euclidean geometry of the old Greeks, which was designed to describe man-made objects. While Euclidean objects (such as squares, cubes, spheres etc.) are invariant under Euclidean symmetry operation (such as rotation or translation), the fractal objects are characterized by a dilation symmetry operation often referred to as self-similarity.

A coastline is a classical example of a fractal object. As you zoom in on it from above, smaller and smaller bays and headlands appear. Consequently, fractals lack characteristic length scale. This contrasts with Euclidean objects which have one, or at most a few, characteristic sizes or *length scales* (e.g., the radius of a circle, or the side of a square). Fractal shapes are scale-independent and are self-similar. Consequently, for a fractal object, the number of features of a certain size $N(\ell)$ (such as the number of bays of a given size along a coastline) varies as ℓ^{-D}, where ℓ is the scale used in the measurement, and D is the fractal dimension of the object.

In mathematical language, we say that $N(\ell)$ *scales* as a *power* of ℓ, and the relation

$$N(\ell) \sim \ell^{-D} \tag{1}$$

is referred to a scaling (or power) law. Its consequence is a statistical distribution of objects (such as tree branches, fjords, pores, cracks) that obey fractal statistics. These distributions have long tails that contrast with bell shaped ('normal') Gaussian functions. Therefore, power law (fractal) distribution functions are more appropriate for description of geological species such as pores, cracks, shales, heterogeneities etc.

The exponent D in (1) is an example of fractal dimension, and it describes quantitatively the degree of irregularity of fractal objects. We shall illustrate the computation of a fractal dimension by the so-called box-counting method for the porespace of a sample of a thin section of porous sedimentary rock. The porespace was viewed through an optical microscope. The image was then digitized and stored in a computer. In Figure 1, we display a typical digitized image, where the white regions represent pores, and the black regions represent grains. In addition, we display in Figure 1 a grid made from boxes of size ℓ_1. We count the number of boxes $N(\ell_1)$ which contain a pore (this can be a whole pore or a fraction of porespace). Then we cover the image with a grid consisting of boxes of size ℓ_2, and count $N(\ell_2)$. This is repeated for various box sizes. Finally, we plot $N(\ell)$ versus ℓ on a doubly logarithmic scale. If the scaling relation (1) holds, then we get a linear plot, where D is given by the negative value of the slope.

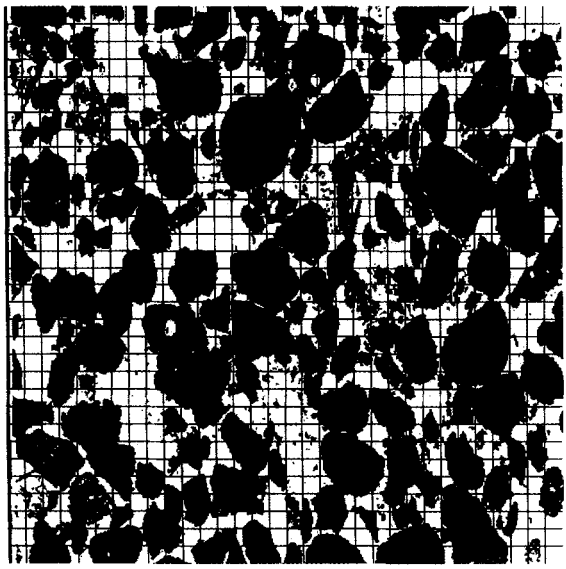

Fig. 1. Digitally displayed porespace (white) in a sandstone covered by a box-counting grid.

In Figure 2, we display digitized pictures of a thin section North Sea sandstone taken at five different magnifications (for details, see [5]). As we zoom in on the sample from (a) till (e), new structure is successively revealed, but the statistical self-similarity (the major characteristic of fractal objects) is retained. This is demonstrated in Figure 3a where we display the log–log plot of $N(\ell)$ versus ℓ *for the five digitized images* in Figure 2. As may be seen, the data for all the five ranges of magnification appear to fall on a straight line with the slope 1.73.

To probe a possible fractal scaling of the pore-grain interface, the same box-counting technique was used. For this, the number of boxes $N(\ell)$ needed to cover *the contours of borderline between black and white regions* in Figure 1 was counted for different box sizes ℓ. The results are shown in the log–log plot of $N(\ell)$ versus ℓ in Figure 3b. Again, it can be seen that the data appear to fall on a straight line with the slope 1.59.

In principle, one should extend this method to three dimensions by counting the number of cubes containing a pore (or its surface). In practice, this is elaborate and requires a sophisticated experimental set-up. Therefore, in this work we concentrate on two-dimensional models in order to gain a basis for understanding the porespace geometry.

One way to obtain a fractal dimension from a three-dimensional sample is to use small angle scattering of either neutrons (SANS) or X-rays (SAXS) from a three-dimensional piece of rock. One can show that both volume and surface fractal dimensions are related to the exponent in a power law relation between scattering intensity and reciprocal number [6]. However, there are often experimental difficulties associated with the scattering method, and the results are not always reliable.

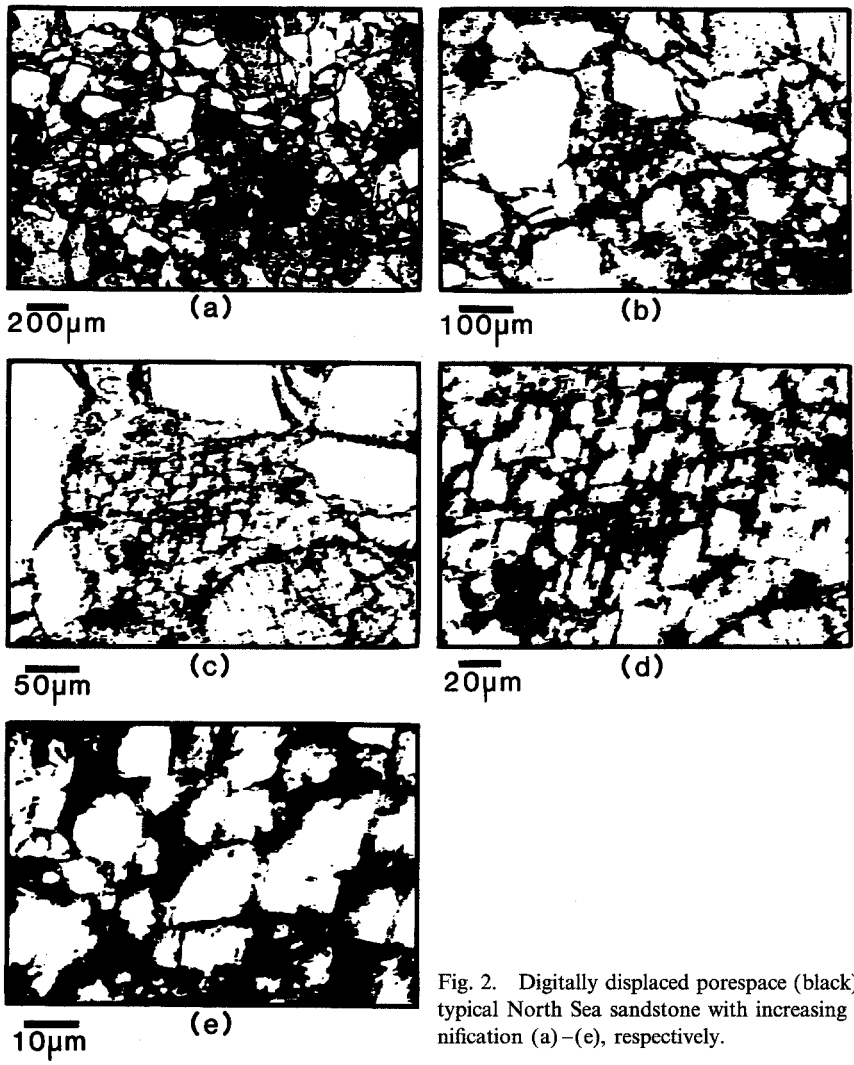

Fig. 2. Digitally displaced porespace (black) in a typical North Sea sandstone with increasing magnification (a)–(e), respectively.

A word of caution! For mathematical fractals constructed by simple algorithms (such as the well-known Cantor set [1]), self-similar behaviour is observed to the zero length scale limit, although the situation is different for fractals in nature. While the zero length scale limit is possible in the mind of a mathematician, for naturally occuring fractals, there are always upper and lower limits between which we observe fractal scaling.

3. Fractal Model of a Sedimentary Rock

The major motivation behind the fractal analysis of porous sedimentary rocks is our belief that the observed scaling behaviour of the porespace of these materials

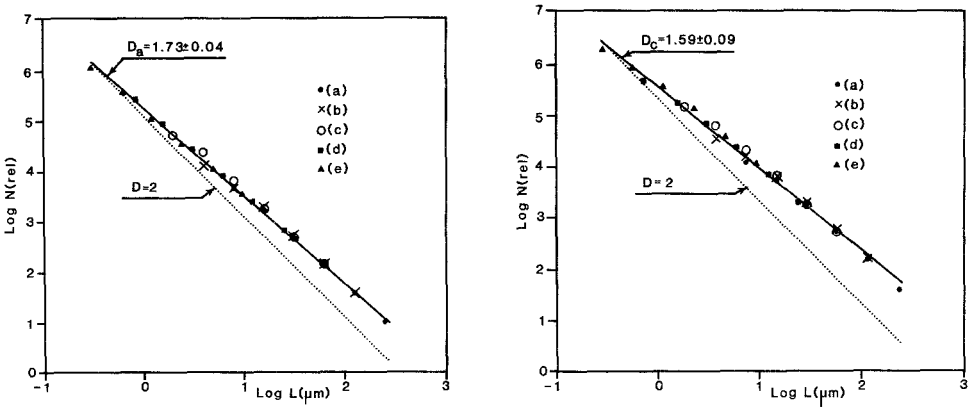

Fig. 3. The fractal dimension D_a of the porespace area and D_c of the contours determined from the log–log plot of the relative number of boxes needed to cover the pores and the contours respectively, versus box size L of the different magnification (a)–(e) in Fig. 2.

can be used to predict their fluid flow characteristics. This is because the flow characteristics of porous media (in particular permeability and conductivity) depend upon the geometry of the porespace. Nonfractal models of flow are likely to lead to the wrong conclusions.

In order to illustrate this idea, we have built a simplified model of a fractal porous medium and have calculated its flow properties. There are several attractive features of the model (see Figure 4), even though the model is a gross oversimplification of the real porespace. In our model, the largest pore empties into N_1 smaller pores each of diameter ℓ_1, which empty into N_2 pores of diameter ℓ_2, and so on. Here, we not only organize the pores unto a fractal hierarchy (a tree [11]), we also assume that the rock has the geometry of the tree (see Figure 4). This latter assumption is unrealistic, but it has the realistic feature that (a) the model porespace is fractal, and (b) the flow is always limited by the *smallest* pores: there is no path through this model rock that avoids passage through the smallest pores.

The motivation behind these features is simple. Looking carefully at the porespace of a sedimentary rock, we often see that the porespace regions are disconnected in such a way that there is *no connected* path through the rock via the pores that are seen. This means that the actual connections are formed by the smallest pores; those smaller than photographic resolution (e.g., see Figure 1). Hence, the permeability is always limited by the flow through the smallest pores in the rocks. In addition we now *know* that porespace statistics are multifractal (see Section 4). Therefore, fractal models of transport are required.

Adler [7a, b] has described the flow properties of a fractal model based on the well-known Sierpinski carpet. The major drawback of his model is that the liquid flow is *not* limited by the flow through the smallest pores. In fact, in Adler's model, the fluid flow has the connectivity provided by the largest pores. Though pedagogically instructive by clearly indicating the scaling behaviour of porespace, Adler's

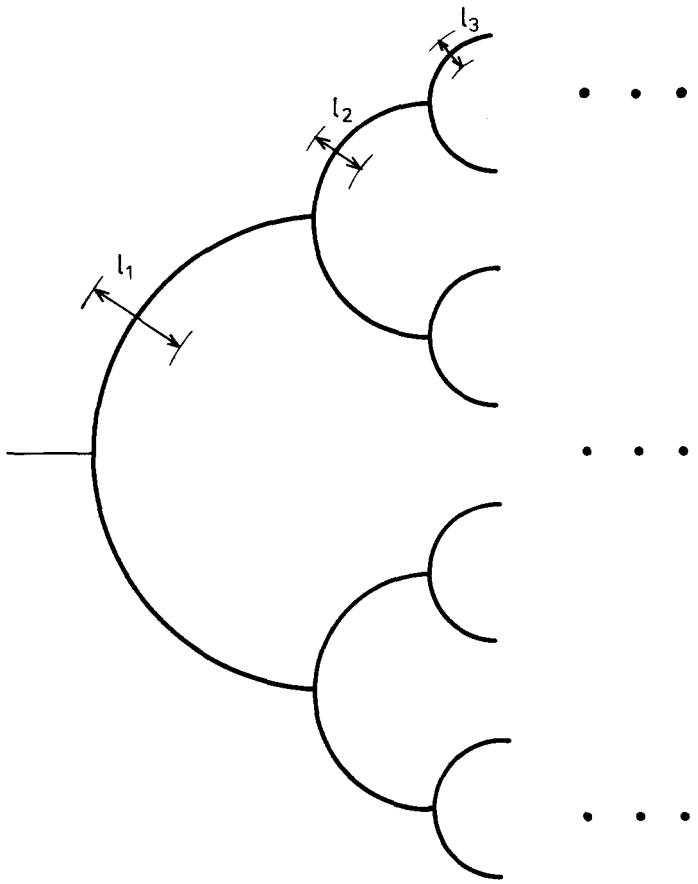

Fig. 4. Oversimplified, but fractal model of a porous rock.

rock model cannot describe correctly the flow properties of the sample in Figure 1. The models of Wong *et al.* [8], and of Katz and Thompson [9], do not suffer from the same defect, as they are based upon arguments of diagenesis leading to a zero-percolation threshold. However, the model of Wong *et al.* uses Gaussian statistics, and Katz and Thompson's empirical model (also nonfractal) lacks a theoretical basis. The strength of our model is that it incorporates the right statistics from the start, albeit in an easy and naive way, and that it also suggests how it can be done correctly along lines qualitatively similar to those of [8].

It is easy to compute the electrical resistance of our model. In generation n, each branch of the tree (pore) has a fixed length L and a cross-section area $A_n \sim \ell_n^2$ (see Figure 4), where $\ell_n \sim a^{-n}$, and so it contributes a resistance $R_n \sim \ell_n / A_n \sim \ell_n^{-2} \sim a^{2n}$ to the circuit. For an octal tree ($N_n = 2^{3n}$), the resistance of the circuit (tree) is

$$R \sim 2^3 \sum_{i=1}^{n} \ell_i^{-2} / 2^{3i} - \frac{2^3 (a^2/2^3)^n}{1 - 2^3/a^2} . \tag{2}$$

The porosity Φ is proportional to the total volume v_n occupied by all the branches through which fluid flows,

$$v_n \sim \sum_{i=1}^{n} 2^{3i} \ell_i^2 \sim \frac{a^2/2^3}{a^2/2^3 - 1}, \tag{3}$$

so that with

$$v_T \sim 2^{3n} a^2 (2^3 - 1)^{-1}, \qquad \Phi = v_n / v_T, \quad \text{and} \quad D = \log 8 / \log a,$$

$$\ln R / \ln \Phi \sim (D-2)/D, \tag{4}$$

where D is the fractal dimension of our model. Conductivity G is given by the reciprocal of resistance ($G = 1/R$), yielding

$$G \sim \Phi^{(2-D)/D} = \Phi^m, \tag{5}$$

so that the Archie's law exponent is

$$m = (2 - D)/D, \quad \text{where } 1 < D < 2.$$

To obtain the permeability k, we start from the assumption that the flow rate through a tube with radius r is given by

$$q = r^4 \mid \nabla P \mid \mu \sim r^4. \tag{6}$$

Replacing an electrical resistance R in (2) by flow, and knowing that the permeability of a single-tube element $k_n \sim \ell_n^4$, we arrive at

$$k \sim \Phi^{(4-D)/D}, \tag{7}$$

which is an example of a Kozeny equation.

It is interesting to note that the conductivity and permeability exponents in the Archie and Kozeny equations (5) and (7) respectively, are *determined entirely by the fractal dimension D* of the pore-space in this approximation. Jacquin and Adler [7b] derived a corresponding result for permeability with a different exponent $(4-D)/(2-D)$ in equation (7) for a model where the largest pores provide the porespace connectivity. The work of Adler and co-workers [7c] has not been extended to three-dimensional models of porous rocks.

Our model, based upon flow through the smallest pores in a complete binary tree, predicts an exponent in Equation (5) between 0 and 1. Since we force the flow through the smallest pores, one would expect that our exponent should be an upper limit on real exponents, where larger pores might provide some short-circuiting. Measurements, however, yield exponents that are larger than ours. How to account for the discrepancy? The point is, that the fluid has even more resistance to the flow than we predict, based upon a highly constricting model. One way to make our model even more constricting would be to systematically prune entire branches from the binary tree. Whether this leads to a larger exponent, or merely a prefactor, must be answered by further research.

In order to make a more realistic model of a porous rock, we introduce the concept of multifractal scaling. This will be done in the next section.

4. Multifractional Scaling in Sedimentary Rocks

A natural question to ask is whether there is only one exponent which describes a scaling behaviour of a fractal? In fact, it turns out that there exists a whole sequence of scaling exponents, which characterize fractal objects, and the above discussed fractal dimension D is only one of them. Therefore, one talks about multifractal scaling or multifractals. Originally designed to describe scaling behaviour of a singular distribution of density [1], multifractal analysis can be generalized (see [10] and [11]) to describe the scaling of nonuniform fractal objects occurring in nature as well as those generated on a computer by recursive algorithms. The beauty of multifractal concepts is that they provide a means for *organizing* often complex and bewildering phenomena such as turbulence, diffusive growth, transport properties of percolating systems, and, as we shall demonstrate, the porespace structure in sedimentary rocks. Lovejoy and Schertzer [14] have already pointed out that many geophysical fields such as radar reflectivity fields generated by showers, cloud fields, mountain fields and others can be successfully characterized by multifractal functions. Sreenivassan [15] and co-workers have observed multifractal scaling of energy-dissipation fields in turbulent flows. The multifractal formalism has given us new tools for extracting order from apparent randomness (disorder) in nature. Further, a multifractal distribution with positive $f(\alpha)$ is a sign of deterministic chaos (see [2], [10] and [11]).

We shall not try to give a detailed description of our approach to multifractals. For this, we refer the reader to [2], [10] and [11]. Instead, we shall give a brief outline of *one way* that we can talk about them, especially within the context of rock characterization: we organize the porespace into an hierarchy of generations of different characteristic pore sizes.

We refer back to Figure 1, where we display a digitized image of the porespace covered by N_n boxes of size ℓ_n, and where the subscript n indicates the nth generation scale. We associate the contents of each box with the fraction P_i of the total porespace it contains. The generating function χ defines the multifractal scaling in terms of the scaling exponents α and $f(\alpha)$, and is given by

$$\chi(q) = \ell_n^{q\alpha - f(\alpha)}, \tag{8}$$

and can be calculated from porespace statistics by using

$$\chi(q) = \sum_{i=1}^{N_n} P_i^q. \tag{9}$$

The quantities α and $f(\alpha)$ are given according to the equation

$$\alpha = \tau'(q) = \frac{1}{\ln \ell_n} \left(\sum_{i=1}^{N_n} p_i^q \ln P_i \right) \Big/ \sum_{i=1}^{N_n} p_i^q \tag{10}$$

and the Legendre transformation

$$f(\alpha) = q\alpha(q) - \tau(q), \tag{11}$$

where

$$\tau(q) = \frac{1}{\ln \ell_n} \ln \left(\sum_{i=1}^{N_n} p_i^q \right). \tag{12}$$

The procedure for calculating α and $f(\alpha)$ is carried out for n refinements of coarsegraining with q ranging usually from $q_{\min}$ (ca. -15) to $q_{\max}$ (ca. 15) with steps of 0.1. Note that a given value of q fixed α through (10), and $f(\alpha)$ through (11) and (12).

The experimental procedure for digital analysis of rock samples has been described in [5]. Briefly, the rock samples were polished thin sections (thickness 30 μm) bound to a glass substrate. The images were digitized using a videoframe grabber with 512×512 pixel resolution. The $f(\alpha)$ curves were determined, using a box-counting computer program based on multifractal theory, described in Equations (8)–(12). The range where the multifractal scaling is valid was found to be in the region from 16 to 128 pixels with $n = 4$ generation scales. Our lower limit of 16 pixels is not due to the sizes of the smallest grains, but due to the limit of resolution of our photographs.

In Figure 5, the $f(\alpha)$ spectra corresponding to three different sedimentary rocks from Zaire (very fine sand, medium fine sand and chalk, with porosity 27%, 23% and 17% respectively, and permeability 1585 md, 2975 md and 177 md respectively) are shown. The standard deviation error bars are based on the statistics from ten different images taken arbitrarily from the same thin section. *Note that the difference in texture of the three samples is reflected in the shape of the $f(\alpha)$ curves.*

The form of the curves in Figure 5 agrees with the upwards convex behaviour of an $f(\alpha)$ function [10]. As explained below, we shall be particularly interested in its two end points $[\alpha_{\min}, f(\alpha_{\min})]$, $[\alpha_{\max}, f(\alpha_{\max})]$, and its maximum $f_{\max}(\alpha)$.

Multifractal behaviour occurs whenever scaling is observed for more than one first-generation length scale. The simplest multifractal is a two-scale Cantor set (see Figure 6a). If its two scales ℓ_1 and ℓ_2 are equal (see Figure 6a(a)), then the resulting one-scale Cantor set possesses a trivial $f(\alpha)$ spectrum which is just a point (see Figure 6b). In this case all the α and $f(\alpha)$ exponents are equal to one number D. We also note [10] that the maximum $f_{\max}(\alpha)$ of a nontrivial $f(\alpha)$ curve is equal to the box-counting exponent D. Thus the box-counting described in Section 2 yields a peak for the $f(\alpha)$ curve $f_{\max}(\alpha) = D$. In many cases, this number can be very similar for entirely different rock textures, and therefore a full multifractal analysis with its $f(\alpha)$ spectrum is a step forward in the direction of more accurate rock characterization.

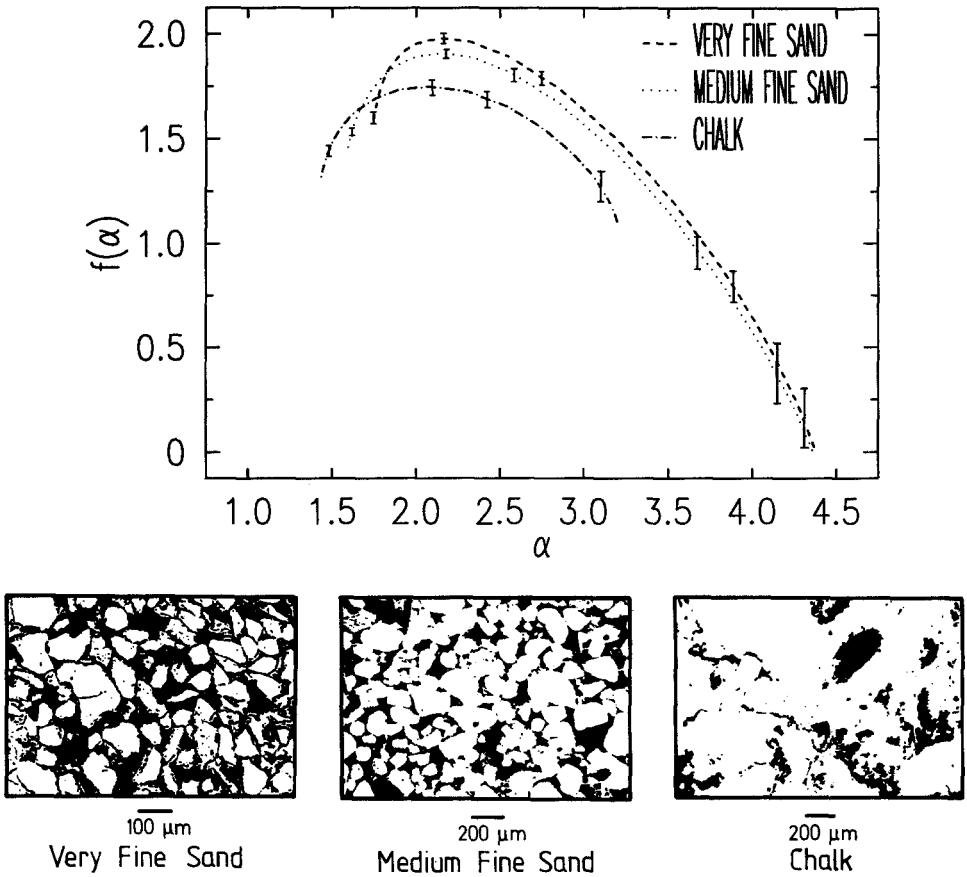

Fig. 5. The $f(\alpha)$ spectra for three different sedimentary rocks reflect different texture of the rocks.

This is clearly illustrated in Figure 6, where we display four different two-scale Cantor sets and their $f(\alpha)$ spectra. We note that the different texture of each set is reflected in the details of the $f(\alpha)$ curves. To illustrate the point, we have chosen the sets in such a way that they all have identical $f_{\max}(\alpha)$ values.

In order to model the rock, we introduce a natural eight-scale generalization of the Sierpinski carpet. Qualitatively, it is an eight-scale Cantor-like set in the plane, and we introduce it by defining the model-generating function

$$\chi(q) = \left(\sum_{i=1}^{8} P_i^q \right)^n \simeq \ell_n^{q\alpha - f(\alpha)}, \tag{13}$$

where $\Sigma_{i=1}^{8} P_i = 1$, and there are eight first-generation scales $\ell_i \leqslant 1/3$ (cf. Figure 7a). The usual one-scale Sierpinski carpet [1] follows from setting $P_i = 2^{-3}$; $\ell_i = 3^{-1}$ (cf. Figure 7b).

In the interest of simplicity, we attempt to model our empirical $f(\alpha)$ curves by the simplest possible case, the two-scale Sierpinski carpet. In this case, the eight scales

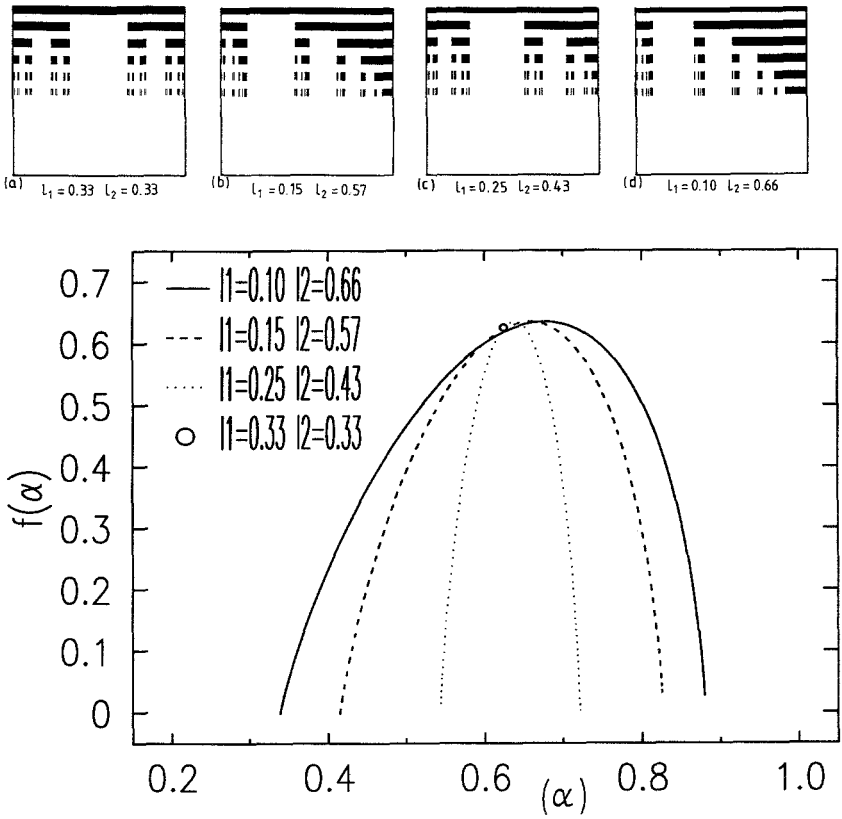

Fig. 6. Geometrical representation of four two-scale Cantor sets with (a) different scaling ratios ℓ_1 and ℓ_2, and (b) their corresponding $f(\alpha)$ spectra.

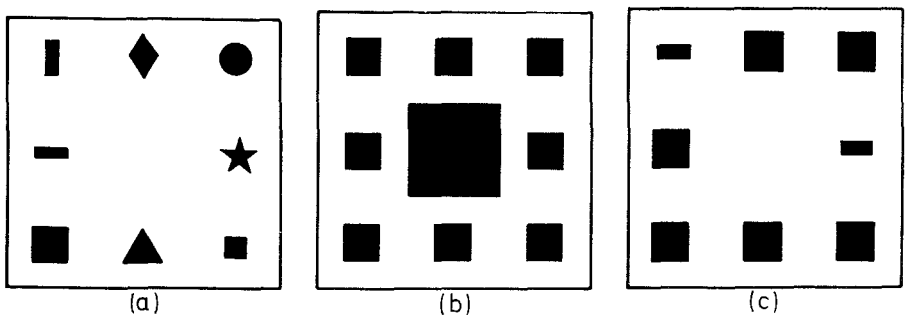

Fig. 7. In all the figures, the dark regions represent pores, the white regions sandgrain. (a) The first generation of the eight-scale generalization of the Sierpinski Carpet. The hierarchy is octal, so that each nth generation pore gives birth for eight new $(n+1)$st generation pores. ℓ_i is the width of the ith pore and P_i is the fraction of the total area occupied by that pore in the nth generation. (b) An example of the first stage of recursion of the (one-scale) Sierpinski carpet. (c) Here $b = 2$, so that six of the eight scales are equal to ℓ_1; the other two are equal to ℓ_2 in the first generation.

ℓ_i collapse into only two, ℓ_1 and ℓ_2 (cf. Figure 7c), and Equation (13) reduces to

$$\chi(q) = (bP_1^q + (8-b)P_2^q)^n, \tag{14}$$

where $bP_1 + (8-b)P_2 = 1$, with $1 \leqslant b \leqslant 7$. Thus, in our model we have set b of scales ℓ_1 to ℓ_1, and the other $(8-b)$ scales to ℓ_2. Notice [11] that $\ln P_1 = \alpha_{\min} \ln \ell_1$ so that the determination of any two members of the triplet (P_1, ℓ_1, $\alpha_{\min}$) fixes the third member. The same is true for $\ln P_2 = \alpha_{\max} \ln \ell_2$. Furthermore, in our model [11] $f(\alpha_{\min}) = -\ln b / \ln \ell_1$ and $f(\alpha_{\max}) = -\ln(8-b)/\ln \ell_2$.

If we consider the generating function Equation (13), we can qualitatively interpret the probabilities $P_i \sim \ell_i^{\alpha_i}$ as follows: imagine organizing the porespace into a hierarchy of generations of pore sizes, where there are N_n pores with sizes $\ell_1^{(n)}, \ldots, \ell_{N_n}^{(n)}$ in the n^{th} generation. The larger pores correspond to small n, the smaller ones to large n, and $\ell_1 > \ell_2 > \cdots > \ell_n$ describes the ordering of characteristic scales in the hierarchy. Then $P \sim \ell_n^{\alpha}$ is a fraction of the porespace occupied by a pore with characteristic size ℓ_n and scaling index α, and then there are $N(\alpha) \sim \ell_n^{-f(\alpha)}$ such pores in the n^{th} generation.

We have tested our two-scale model of a porous rock on a multifractal spectrum of a North Sea sandstone. The results of the fit to the experimental data are displayed in Figure 8. The details of the fitting procedure are discussed in more details in [11], however, we note that the fit is reasonable. We performed similar fits

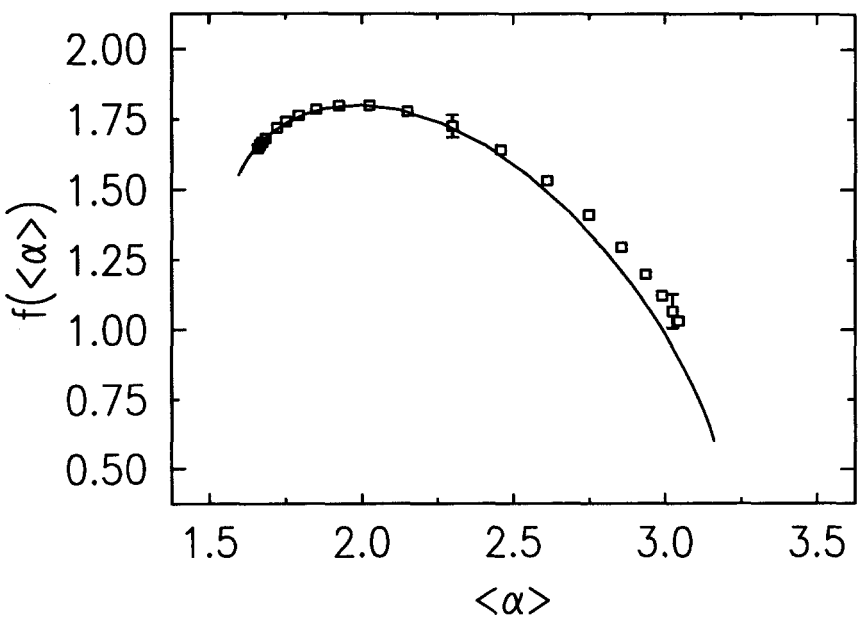

Fig. 8. Direct comparisons of the $f(\langle\alpha\rangle)$ spectra for the two-scale model (solid lines) and the experimental observations for a North Sea sandstone in [11]. The fitted parameter values: $P_1 = 0.141$, $P_2 = 0.013$, $\ell_1 = 0.333$; $\ell_2 = 0.315$, $b = 7.0$. The $\langle\ \rangle$ parantheses indicate that we have chosen the canonical formalism for $f(\alpha)$. For further details on this choice see [2] and [11].

Table I. Numerical values of P_1, P_2, ℓ_1, ℓ_2 and b obtained from the fit of Equations (13) and (14) to the experimental $f(\alpha)$ spectrum for the three rocks displayed in Figure 5

Rock type	P_1	P_2	ℓ_1	ℓ_2	b
Very fine sand	0.16	0.02	0.34	0.35	6
Medium fine sand	0.18	0.04	0.33	0.33	5
Chalk	0.18	0.03	0.30	0.31	5

to the curves in Figure 5. The results of these fits in terms of P_1, P_2, ℓ_1, ℓ_2 and b are given in Table I. Thus, the interesting feature of this study is that we have managed to express quantitatively the scaling behaviour of the porespace of a sedimentary rock in terms of five free parameters.

It seems natural to make use of the scaling hierarchy of the generation of pores sizes to build a more realistic permeability model of a porous rock than the oversimplified model described in Section 3. This is not a trivial task, and in the following, we just give an outline of one way to tackle this problem.

As in Section 3, the idea is to compute the electrical circuit model with each resistance given by $R_i = \ell_i / A_i$, where ℓ is a length and A a cross-section area. We have argued that in our model of a porous rock the area A_i is equal to a fraction of porespace $P_i \sim \ell_i^{\alpha_i}$, occupied by a pore with characteristic size ℓ and scaling index α.

To construct the circuit, we propose to use the two-dimensional photo of the thin slice of porous rock (Figure 1), and replace pores by resistors in the following way: the largest pores are replaced by resistors with magnitude $R_{1,i} \sim \ell_i^{(1)\,1-\alpha_i}$, where $\{\ell_i^{(1)}\}$ is the set of first-generation length scales. The procedure is continued, replacing the pores in the next generation of sizes by resistances $R_{2,i} \sim \ell_i^{(2)\,1-\alpha_i}$, where $\{\ell_i^{(2)}\}$ denotes the second generation of pore size scales. The connections are to be made according to the photo of Figure 1, and the missing small pores are filled in by adding the highest resistances in a way that reflects their multifractal scaling. In fact, the entire network, by construction, should agree with the model $f(\alpha)$ curve. To the best of our knowledge, no one has previously attempted to model the conductivity network of the rock in this particular way. Once the network has been constructed, standard methods of analysis should be applicable for extracting the conductivity and permeability [12]. In the end, the extent within which the permeability can be predicted in two and especially three dimensions will be limited by computer time. Presently, we try to investigate [13] whether such a realistic network can be replaced by an approximate but simpler one (e.g., a model based on Effective Medium Theory) that permits the extraction of some useful analytic results.

5. Concluding Remarks

In this work, we have tried to emphasize the usefulness of the recent developments in condensed matter physics and nonlinear dynamics in tackling a complex problem

such as fluid flow through a sedimentary rock. We have not presented a final solution to the problem, but have indicated the path that we propose to take.

The idea is based upon exploiting the scaling property of *rock's pore geometry* with the help of fractal statistics. As the first step, we have built a simple model with only one scaling exponent. Even at this level of simplicity, the model reproduces the well known empirical Archie and Carman–Kozeny equations known to reservoir engineers for many years.

We have used the idea of multifractal scaling to characterize samples of rock with different textures by their multifractal $f(\alpha)$ spectrum. We have introduced a two-scale Cantor-like model, which generates a similar porespace distribution and which provides analytic $f(\alpha)$ curves which fit to the measured results. We have proposed how this model can be used to extract permeabilities and conductivities of the given rock samples.

Multifractal scaling is a tool for extracting a certain amount of order and correlation from apparently random systems. It would be of interest to test these ideas in extracting both order and space correlation from well-log data of permeabilities, porosities and other petrophysical quantities of interest. This seems plausible in particular for the permeability data, which usually follow log-normal distributions. Such distributions have tendencies to have long tails which are characteristic of fractal statistics. These ideas are currently being tested.

Acknowledgements

We would like to thank A. T. Skjeltorp of the Institutt for energiteknikk (IFE) and F. de Silva of Petrofina for valuable comments, discussions and encouragement. We also thank A. T. Skjeltorp for providing us with Figures 2 and 3. This work is part of a common project IFE/Fina Exploration Norway/Petrofina.

References

1. Mandelbrot, B., 1982, *The Fractal Geometry of Nature*, Freeman.
2. McCauley, J. L., 1990, *Z. Phys. B.* **81**, 115.
3. Kozeny, J., 1927, Sitzungsber, Akad. Wiss. Wien **136**, p. 271.
   Carman, P. C., 1948, Disc. Faraday Soc. **3**, p. 72.
4. Archie, G. E., 1942, *Trans. AIME.*
5. Hansen, J. P. and Skjeltorp, A. T., 1988, *Phys. Rev. B* **38**, 2635.
6. Wong, P. Z., 1987, in Banavar, J., Koplik, J., and Winkler, K. (eds.) *Physics and chemistry of porous media II, AIP Conference Proc.* **154**, 304–318, American Institute of Physics, New York.

7a. Adler, P. M., 1986, *Phys. Fluids* **29**, 15.
7b. Jacquin, C. G. and Alder, P. M., 1987, *Transport in Porous Media* **2**, 571.
7c. Lemaiter, R. and Alder, P. M., 1990, *Transport in Porous Media* **5**, 325.

8. Wong, P. Z., Koplik, J., and Tomanic, J. P., 1984, *Phys. Rev. B* **30**, 6606.
9. Katz, A. J. and Thompson, A. H., 1986, *Phys. Rev. B* **34**, 8179.
10. McCauley, J. L., 1990, *Physics Reports* **189**, 225.
11. McCauley, J. L., 1989, *Int. J. Modern Phys. B*, 821.

12. Koplik, J. and Lassiter, T. J., 1985, *SPE*, February.
13. Hansen, J. P. and Muller, J., in preparation.
14. Schertzer, D. and Lovejoy, S., 1990, Non-linear variability in geophysics: analysis and simulation, in Pietronero, L., (ed.) *Fractals*, 49–79, Plenum Press.
15. Sreenivassan, K. R., Prasad, R. R., Meneveau, C., and Ramshankar, R., 1989, The fractal geometry of interfaces and multifractal distribution of dissipation in fully turbulent flows, in Scholz, C. H. and Mandelbrot, B. B., (eds.) *Fractals in Geophysics*, Birkhäuser.